Received: Added at production | Revised: Added at production | Accepted: Added at production

DOI: xxx/xxxx

ARTICLE TYPE

A New Continuous Class-E Mode Based on the General Theory of High-Efficiency Continuous Power Amplifier

Xuepeng Wei | Yonglun Luo* | Yulan Wu | Guoqing Yuan | Rong Chang | Guoping Hong

Research Institute of Electronic Science and Technology, University of Electronic Science and Technology of China, Chengdu, China

Correspondence
*Yonglun Luo, Research Institute of Electronic Science and Technology, University of Electronic Science and Technology of China, Chengdu 611731, China.
Email: dlyluo@uestc.edu.cn

Summary

By multiplying with the continuous factor (CF), the conventional Class-F/F^{-1}, Class-J power amplifier (PA) can be expanded to their corresponding continuous modes, resulting in a great degree of freedom for broadband design. However, this method can hardly apply to other types of PAs. In view of this problem, the continuous mode is deeply analyzed from the perspective of equation solving for the first time, and a general theory for high-efficiency broadband continuous PA design is proposed. In this theory, the continuous impedance space does not rely on a mapping relationship achieved by multiplying with the CF, but on a direct solution of the high-efficiency equations to obtain the broadband design space. This approach is simpler and has the potential to provide greater design space. As a validation, this theory is used for the analysis of Class-E PAs and a new continuous Class-E (NC-E) PA is presented. With knee-point voltage and finite harmonics taken into account, this type of PA greatly expands the broadband design space of Class-E PAs, and also has the advantage of harmonic matching. The NC-E PA is designed and manufactured using GaN HEMT CGH40010F, which achieves 40.6∼41.6dBm output power and 66.2%∼74.2% drain efficiency (DE) in the frequency band of 2.5-3.8GHz.

KEYWORDS:
power amplifier, broadband, high-efficiency, linear space, waveform analysis, radio frequency

1 | INTRODUCTION

With the development of technology, radio frequency (RF) PAs play more and more important roles in wireless communication systems. The huge energy consumption and high-speed data transmission rates of the new generation communication system put forward higher requirements for the efficiency and bandwidth of PAs.

1.1 | Basic Theory of PAs

PAs can be divided into two categories according to their operating mode characteristics: switch-mode power amplifiers (SMPAs) and harmonic-tuned power amplifiers (HTPAs).

The Class-E PAs is a typical representative of SMPAs. Traditional Class-E PAs made up of lumped elements are not applicable in RF band, and transmission lines have been introduced into the matching network to solve this problem. But this theory can often control second and third harmonics only [1,2,3]. These designs are actually based on approximate switching modes and harmonic tuning strategies [4,5,6]. The HTPA is another way to achieve high efficiency. The Class-F PA is a widely studied HTPA

with theoretical efficiency of 100% and specific load impedance with infinite harmonics[7]. However, its high-efficiency design space requires to switch back and forth between open and short points, so most Class-F PAs tune harmonics up to the 3rd order with the consideration of circuit complexity[8,9,10].

1.2 | The Continuous Design Theory of PAs and its Limitations

In terms of broadband Class-E design theory, a continuous Class-E (C-E) theory had been proposed[11,12]. The current phase was viewed as a free factor in this theory, resulting in a broadband impedance space switching among Class-EF, Class-E, and Class-E/F. Besides, other explorations on broadband Class-E PAs were often based on Load-Pull techniques[13] or on circuit structure innovations to match the ideal impedance point within the bandwidth[14,6,5].

In terms of broadband HTPA design theory, the continuous mode provides better bandwidth performance and constant efficiency by offering greater design flexibility in fundamental and harmonics[15,16,17,18]. Unlike C-E PAs, the core of continuous Class-F/F^{-1}, Class-J PAs is CF ($1-\gamma sin(\theta)$), which expands a single voltage or current waveform into a series of waveforms through an ingenious multiplicative mapping relationship. These waveforms may deviate from the original waveform in shape, but maintain a constant output efficiency, thus resulting in greater design space in frequency domain.

This mapping relationship is an effective way to achieve broadband design space of PAs. However, the CF has limitations. Firstly, the application scope of the CF is limited. It is known that only Class-J, Class-F/F^{-1} PAs and their derived types can be extended with CF. Secondly, the relationships between the harmonics are not independent when multiplied, resulting in computational complexity. This is also one of the reasons why CF can hardly be applied to other types of PAs. Thirdly, the continuous waveforms obtained by multiplication generally retain some of the characteristics of the original waveform, which may limit the degrees of freedom.

1.3 | The Idea of This Article

Here the continuous theory is analyzed from the perspective of equation solving, and the cluster of waveforms obtained by continuous mode is actually the set of solutions of the high-efficiency equation. With above idea, a new general theory for high-efficiency broadband continuous PA is proposed. This theory is based on the solution of high-efficiency equations rather than the multiplication of CF. With the boundary conditions in time domain and the high-efficiency linear equations in frequency domain, the high-efficiency design space can be can be expressed directly in terms of the solution space of the system of equations. Most importantly, as the type of PA is not specifically designated in analysis, the theory has general applicability.

As a validation, waveforms of Class-E PAs are analyzed. Therefore, a NC-E PA design theory is proposed and its high-efficiency impedance space are given. Unlike the C-E mode derived from circuit parameters, the NC-E PA is obtained with harmonic engineering and continuous method similar to continuous Class-J, Class-F/F^{-1} mode. With knee-point voltage and finite harmonics taken into account, the NC-E PA is actually based on approximate switching modes and harmonic tuning strategies, making it possible to operate at higher frequency bands. Besides, the obtained high-efficiency design space for each harmonic does not require switching back and forth between open and short points, so it has advantages over continuous Class-J, Class-F/F^{-1} PAs in high-order harmonic matching. Finally, the GaN HEMT CGH40010F is used to design and fabricate this type of PA, and the test results show the good performance of the designed PA.

The paper is structured as follows: In Section 2, constraints on achieving continuous PAs are analyzed, thus leading to solving method of general continuous mode. In Section 3, the theory is applied to Class-E PAs and design space for NC-E PAs can be obtained. In Section 4, in order to verify the proposed NC-E PA, circuit design and simulation based on Advanced Design System(ADS) are presented. Then, actual circuit fabrication and measurement are performed in Section 5. At last, conclusions are reached in Section 6.

2 | THEORETICAL ANALYSIS

2.1 | Basic Theoretical Derivation

To obtain the high-efficiency equations and solve them, the basic variables must be defined first. With harmonics up to the fifth order considered, the Fourier decomposition expressions of drain voltage and current waveforms are shown as:

$$V_d(\theta) = \frac{a_{V,0}}{2} + \sum_{n=1}^{5} a_{V,n}\cos(n\theta) + \sum_{n=1}^{5} b_{V,n}\sin(n\theta) \tag{1}$$

$$I_{\mathrm{d}}(\theta) = \frac{a_{I,0}}{2} + \sum_{n=1}^{5} a_{I,n}\cos(n\theta) + \sum_{n=1}^{5} b_{I,n}\sin(n\theta) \tag{2}$$

in which, $a_{V,0}/2, a_{I,0}/2$ are the direct current (DC) components, $a_{V,n}, a_{I,n}(n > 0)$ and $b_{V,n}, b_{I,n}(n > 0)$ are the nth cosine components and nth sine components, respectively.

To simplify the analysis, the current waveform is considered as a fixed value and the continuous voltage waveform is tried to be found in the following. In fact, this assumption is also made in the analysis of continuous Class-F and continuous Class-B/J modes. Assuming that the Fourier decomposition expression of the continuous voltage waveform V_{d_c} is defined as:

$$V_{d\_c}(\theta) = \frac{a_{c,0}}{2} + \sum_{n=1}^{5} a_{c,n}\cos(n\theta) + \sum_{n=1}^{5} b_{c,n}\sin(n\theta) \tag{3}$$

in which $a_{c,0}/2$ is the DC component, $a_{c,n}$, $b_{c,n}(n > 0)$ are the nth cosine components and nth sine components, respectively.

The broadband high-efficiency constraints of the ideal continuous voltage waveform can be expressed as:

- The ideal output efficiency of fundamental is constant and is set as η.
- Harmonics do not consume power.

Transforming the above constraints into frequency domain, we can get following equations:

$$\begin{aligned} P_{1f} &= \eta P_{in} = -\frac{a_{I,1}a_{V,1} + b_{I,1}b_{V,1}}{2} \\ P_{nf} &= -\frac{a_{I,n}a_{V,n} + b_{I,n}b_{V,n}}{2} = 0(n > 1) \end{aligned} \tag{4}$$

where:

$$P_{in} = a_{I,0}a_{c,0}/4 \tag{5}$$

In Equations 4 and 5, P_{1f} is the fundamental output power and P_{in} is the input power. The analysis here is performed under the assumption of finite harmonic tuning, which is closer to the actual design but also results in unavoidable efficiency losses. Based on the above constraints, the dissipation is only caused by the overlap of waveforms[3,8], as:

$$P_{diss} = P_{in} - P_{1f} \tag{6}$$

To make it easier to understand, the waveforms of continuous Class-F mode are given as an example[17], as:

$$\begin{aligned} V_{CF} &= \left(1 - \frac{2}{\sqrt{3}}\cos\theta\right)^2 \cdot \left(1 + \frac{1}{\sqrt{3}}\cos\theta\right) \cdot (1 - \gamma\sin\theta) \\ &= 1 - \frac{2}{\sqrt{3}}\cos\theta - \gamma\sin\theta + \frac{7\gamma}{6\sqrt{3}}\sin 2\theta + \frac{1}{3\sqrt{3}}\cos 3\theta - \frac{7\gamma}{6\sqrt{3}}\cos 4\theta \\ I_{CF} &= \frac{1}{\pi} + \frac{1}{2}\cos\theta + \frac{2}{3\pi}\cos(2\theta) \end{aligned} \tag{7}$$

Substituting the components in Equation 7 into Equations 4 and 5, we can get:

$$\begin{aligned} P_{1f} &= -\frac{a_{I,1}a_{V,1} + b_{I,1}b_{V,1}}{2} = -\frac{\frac{1}{2} \times \left(-\frac{2}{\sqrt{3}}\right) + 0 \times (-\gamma)}{2} = \frac{1}{2\sqrt{3}} \\ P_{nf} &= -\frac{a_{I,n}a_{V,n} + b_{I,n}b_{V,n}}{2} = 0 (n > 1) \\ \eta &= \frac{P_{1f}}{P_{in}} = \frac{\frac{1}{2\sqrt{3}}}{\frac{1}{\pi}} \approx 0.907 \end{aligned} \tag{8}$$

where we can see that the voltage waveform of the continuous Class-F mode varies with γ, but the efficiency remains constant. This is the fundamental reason why continuous modes are able to expand bandwidth. In other words, the cluster of continuous waveforms can be considered as the solution set of Equation 4. Besides, the range of γ is set from -1 to 1 to satisfy the inherent conditions of the PAs, which will be discussed in the next subsection.

The solution of the Equation 4 is performed in the following. As the current waveform is assumed to be fixed, the unknowns in Equation 4 are only $a_{c,n}$, $b_{c,n}$. Subsequently, it is easy to conclude that the Equation 4 is a system of linear non-homogeneous equations. Its solutions contain general solutions (G-solutions) and special solutions (S-solution).

With harmonics up to the 5th order are considered, the S-solutions could be obtained by analyzing the initial waveform in Equation 1, as:

$$Sol_s = [a_{V,0}\ a_{V,1}\ a_{V,2}\ a_{V,3}\ a_{V,4}\ a_{V,5}\ b_{V,1}\ b_{V,2}\ b_{V,3}\ b_{V,4}\ b_{V,5}]^T \tag{9}$$

And Equations 4 contains a total of five equations, resulting in five linearly independent G-solutions. They can be written in the form as:

$$\begin{aligned} Sol_{g1} &= \left[0\ a_{g,1}\ 0\ 0\ 0\ 0\ b_{g,1}\ 0\ 0\ 0\ 0\right]^T \\ Sol_{g2} &= \left[0\ 0\ a_{g,2}\ 0\ 0\ 0\ 0\ b_{g,2}\ 0\ 0\ 0\right]^T \\ Sol_{g3} &= \left[0\ 0\ 0\ a_{g,3}\ 0\ 0\ 0\ 0\ b_{g,3}\ 0\ 0\right]^T \\ Sol_{g4} &= \left[0\ 0\ 0\ 0\ a_{g,4}\ 0\ 0\ 0\ 0\ b_{g,4}\ 0\right]^T \\ Sol_{g5} &= \left[0\ 0\ 0\ 0\ 0\ a_{g,5}\ 0\ 0\ 0\ 0\ b_{g,5}\ \right]^T \end{aligned} \tag{10}$$

in which, $a_{g,n}$, $b_{g,n}$ are the nth cosine component and the nth sine component of the voltage G-solution, respectively. Therefore, the solution of the continuous voltage waveform can be expressed as:

$$Sol = Sol_s + \sum_{n=1}^{5} \lambda_n Sol_{gn} \tag{11}$$

$$Sol = [a_{c,0}\ a_{c,1}\ a_{c,2}\ a_{c,3}\ a_{c,4}\ a_{c,5}\ b_{c,1}\ b_{c,2}\ b_{c,3}\ b_{c,4}\ b_{c,5}]^T \tag{12}$$

where λ_n are free variables. From linear algebra theory, it can be concluded that different values of λ_n will affect the shape of the voltage waveform and the impedance space of the design, while maintaining a constant efficiency.

2.2 | Restrictions in Time Domain

The realizability of the waveform in time domain also needs to be met. The constraints in time domain can be obtained from the inherent conditions of the PAs, as shown below:

$$\begin{aligned} &\min\left(V_d(\theta)\right) \geq 0 \\ &\max\left(V_d(\theta) \leq V_{break}\right. \end{aligned} \tag{13}$$

in which, V_{break} is the breakdown voltage of the transistor.

2.3 | Solution of Continuous Impedance Space

The effects of λ_n on fundamental and harmonic impedances need to be explored. Based on Equations 9-12, the solution of the linear equation can be obtained:

$$\begin{aligned} a_{c,n} &= a_{V,n} + \lambda_n a_{g,n} \\ b_{c,n} &= b_{V,n} + \lambda_n b_{g,n} \end{aligned} \tag{14}$$

In the design of RF PAs, the impedance space of fundamental is the most important, which will be analyzed first. The fundamental impedance can be calculated with components in frequency domain, as:

$$Z_{1,f} = -\frac{a_{c,1} + jb_{c,1}}{a_{I,1} + jb_{I,1}} \tag{15}$$

Then the real and imaginary parts of the fundamental impedance are calculated as:

$$\begin{aligned} \text{real}\left(Z_{1,f}\right) &= -\frac{a_{I,1}a_{c,1} + b_{I,1}b_{c,1}}{{a_{I,1}}^2 + {b_{I,1}}^2} \\ &= -\frac{a_{I,1}\left(a_{V,1} + \lambda_1 a_{g,1}\right) + b_{I,1}\left(b_{V,1} + \lambda_1 b_{g,1}\right)}{{a_{I,1}}^2 + {b_{I,1}}^2} \\ &= -\frac{a_{I,1}a_{V,1} + b_{I,1}b_{V,1}}{{a_{I,1}}^2 + {b_{I,1}}^2} = \frac{2P_{1f}}{{a_{I,1}}^2 + {b_{I,1}}^2} \end{aligned} \tag{16}$$

$$\begin{aligned} \text{imag}\left(Z_{1,f}\right) &= -\frac{a_{I,1}b_{c,1} - b_{I,1}a_{c,1}}{{a_{I,1}}^2 + {b_{I,1}}^2} \\ &= -\frac{a_{I,1}\left(b_{V,1} + \lambda_1 b_{g,1}\right) - b_{I,1}\left(a_{V,1} + \lambda_1 a_{g,1}\right)}{{a_{I,1}}^2 + {b_{I,1}}^2} \end{aligned} \tag{17}$$

It is found from Equations 14, 15 that $real(Z_{1,f})$ remains unchanged with λ_1, while $imag(Z_{1,f})$ is related to λ_1. A similar process can be conducted to obtained the relationship for harmonics. And it is found:

$$\begin{aligned} \text{real}\left(Z_{\text{n},f}\right) &= \begin{cases} \frac{2P_{1f}}{a_{I,1}^2 + b_{I,1}^2}(n=1) \\ 0(n>1) \end{cases} \\ \text{imag}\left(Z_{n,f}\right) &= f_n\left(\lambda_1, \lambda_2 \ldots, \lambda_n\right) \end{aligned} \tag{18}$$

However, in practice, the $\lambda_n(n \geq 2)$ are not independent. After λ_1 has been determined, only a set of optimal $\lambda_n(n \geq 2)$ that can satisfy the constraints is required. That is, the optimal $\lambda_n(n \geq 2)$ can be determined by λ_1, as:

$$\begin{aligned} \text{real}\left(Z_{\text{n},f}\right) &= \begin{cases} \frac{2P_{1f}}{a_{I,1}^2 + b_{I,1}^2}(n=1) \\ 0(n>1) \end{cases} \\ \text{imag}\left(Z_{n,f}\right) &= f_n\left(\lambda_1\right) \end{aligned} \tag{19}$$

There are various ways to find the optimal $\lambda_n(n \geq 2)$, and the nonlinear programming idea is a feasible method. This approach maximizes $\min\left(V_d(\theta)\right)$ to reduce the clipping effect on the current waveform caused by the knee-point voltage [19]. In practice, we use Matlab's $fmincon$ function to perform the process, which is also used in the analysis in Section 3.

Consider the range of λ_n to simplify the solution. For any PA, its fundamental and harmonic amplitudes must be within a certain range, as:

$$\sqrt{a_{\text{c,n}}^2 + \text{b}_{\text{c,n}}^2} \leq k_n\left(V_{DC} - V_{\text{knee}}\right) \tag{20}$$

The values of k_{n} only need to be in the approximate range to accelerate the solving process, if so, they have no impact on the final results. For almost any high-efficiency waveform of PAs, the following values are sufficient:

$$\begin{aligned} k_{\text{n}} &= 3(\text{n} = 1) \\ k_{\text{n}} &= 1.5(2 \leq \text{n} \leq 3) \\ k_{\text{n}} &= 0.75(4 \leq \text{n} \leq 5) \end{aligned} \tag{21}$$

Based on the above analysis, solving process is established as follows: When λ_1 is determined, if a optimal set of $\lambda_n(n \geq 2)$ can be found with Equations 4, 13, then it is considered the solution exists at λ_1. The flowchart of the high-efficiency linear space solution process is shown in Figure 1.

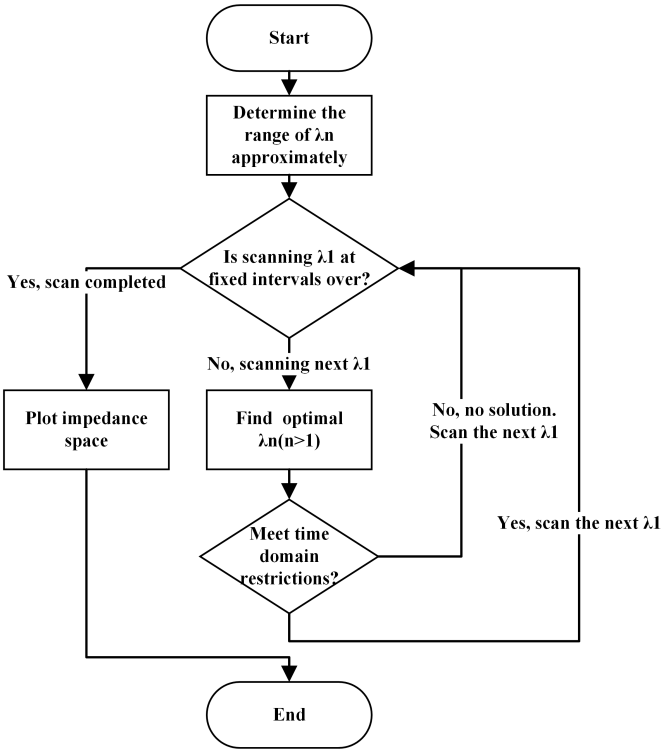

Figure 1 The flowchart of the high-efficiency linear space solution process

3 | APPLICATION AND PRACTICE OF THE THEORY

To verify the feasibility of the foregoing theory, it is applied to broadband expansion of Class-E PAs. The waveform of the Class-E PA previously proposed[20] is used as the initial waveform. The conduction angle is chosen to be 180 degrees and the waveforms are shown in Figure 2 (a). Fourier decomposition is performed on the waveforms with additional consideration of knee-point voltage[8,18], as:

$$\begin{aligned} V_{norm}(\theta) &= \frac{V_d(\theta)}{V_{DC} - V_k} = \frac{a_{V,0}}{2} + \sum_{k=1}^{5}(a_{V,k}\cos(k\theta) + b_{V,k}\sin(k\theta)) \\ I_{norm}(\theta) &= \frac{I_d(\theta)}{I_{DC}} = \frac{a_{I,0}}{2} + \sum_{k=1}^{5}(a_{I,k}\cos(k\theta) + b_{I,k}\sin(k\theta)) \end{aligned} \tag{22}$$

Class-E PAs' waveforms with harmonics up to the fifth order are shown in Figure 2 (b), and the specific values of the sine and cosine components are shown as:

$$\begin{array}{ll} a_{V,0} = \frac{2V_{DC}}{V_{DC}-V_{knee}} & a_{I,0} = 2 \\ a_{V,1} = 0.4674, b_{V,1} = 1.5708 & a_{I,1} = 0.5000, b_{I,1} = -1.422 \\ a_{V,2} = -0.6667, b_{V,2} = 0.5236 & a_{I,2} = -0.3333, b_{I,2} = -0.4244 \\ a_{V,3} = -0.2222, b_{V,3} = 0 & a_{I,3} = 0, b_{I,3} = -0.2122 \\ a_{V,4} = -0.1333, b_{V,4} = 0.0524 & a_{I,4} = -0.0667, b_{I,4} = -0.1698 \\ a_{V,5} = -0.0800, b_{V,5} = 0 & a_{I,5} = 0, b_{I,5} = -0.1273 \end{array} \tag{23}$$

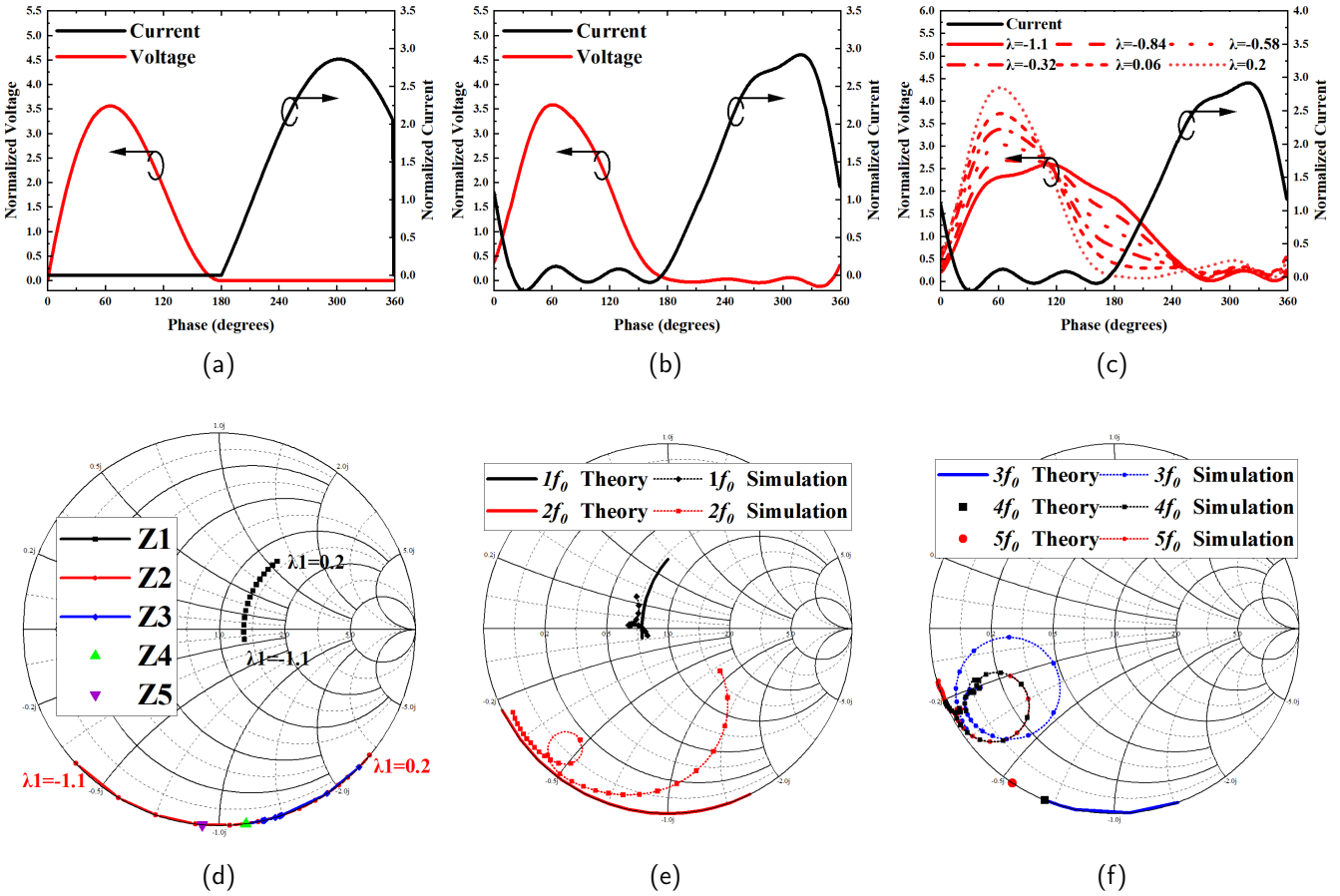

Figure 2 (a) Class-E waveforms with infinite harmonics. (b) Class-E waveforms with harmonics up to the fifth order. (c) NC-E waveforms with harmonics up to the fifth order. (d) Theory fundamental and harmonic impedances of NC-E PAs at the intrinsic drain plane ($Z_0 = R_{opt}$). (e) Fundamental and 2nd harmonic impedances at the intrinsic drain plane ($Z_0 = 50\Omega$). (f) 3rd, 4th, 5th harmonic impedances at the intrinsic drain plane ($Z_0 = 50\Omega$).

Fourier components of the initial voltage waveform are also considered as the high-efficiency S-solution. Combine Equations 4, 23, the G-solutions can be obtained:

$$\begin{aligned} a_{g,1} &= 0.9434, \quad b_{g,1} = 0.3317 \\ a_{g,2} &= -0.7864, \quad b_{g,2} = 0.6177 \\ a_{g,3} &= -1, \quad b_{g,3} = 0 \\ a_{g,4} &= -0.9308, \quad b_{g,4} = 0.3655 \\ a_{g,5} &= 1, \quad b_{g,5} = 0 \end{aligned} \tag{24}$$

As the knee-point voltage has been considered in the above analysis, the high-efficiency impedance space cannot be solved directly without specifying this value. For general FET devices, $V_{knee} \approx 0.2\, V_{DC}$ [19], thus we can probably assume that:

$$a_{V,0} = \frac{2V_{DC}}{V_{DC} - V_k} = 2.5 \tag{25}$$

For the specified device, $a_{V,0}$ can also be recalculated to obtain a more accurate result. In general, the knee-point voltage can have a negative impact on the efficiency. Here, this non-ideal factor also helps to shape the drain voltage waveform to satisfy the time domain condition in Equation 13.

Due to the relatively small impacts on the final results, the values of $\lambda_n (n \geq 4)$ are set to 0 here to simplify matching complexity. With the flow chart in Figure 1 and Equations 13, 20, 23-25, the obtained normalized continuous waveforms of the NC-E PA is shown in Figure 2(c) and the high-efficiency design space is shown in Figure 2(d). The range of λ_1 is determined by the

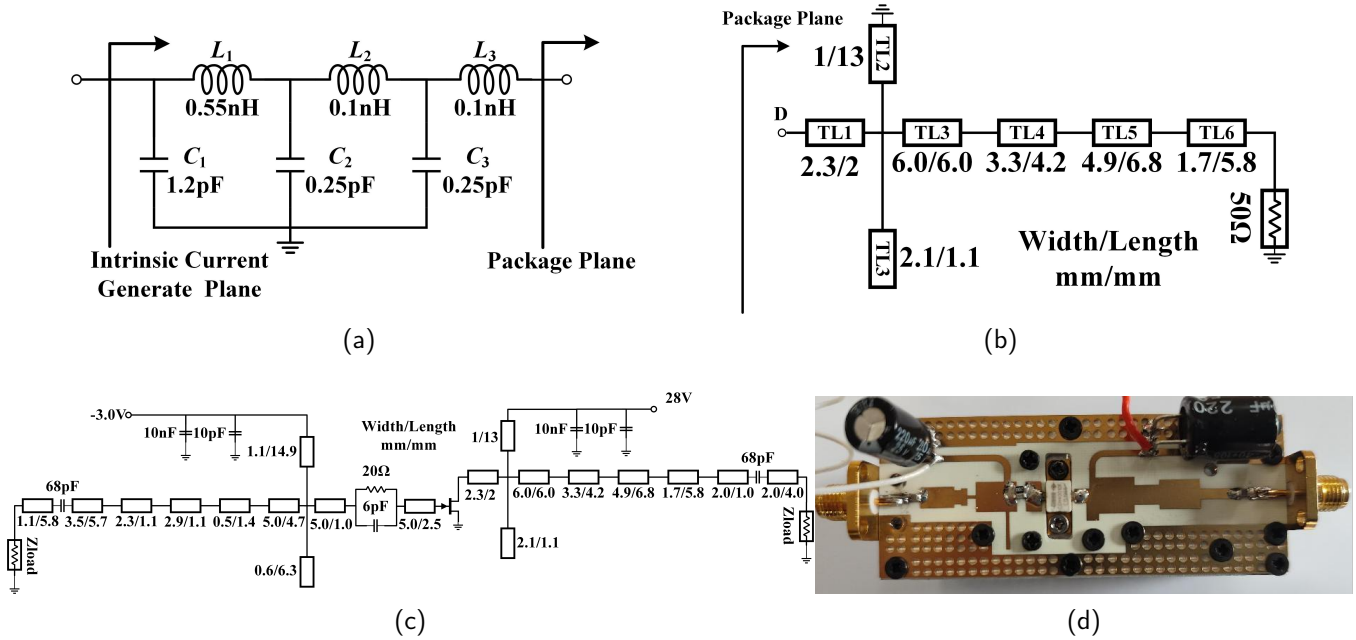

Figure 3 (a) The parasitic parameters of the transistors. (b) The designed output matching circuit. (c) The NC-E PA's circuit schematic. (d) The Fabricated wideband high-efficiency NC-E PA.

flowchart as in Figure 1, and the final result is $-1.1 \leq \lambda_1 \leq 0.2$. From Figure 2(d), we can see that all harmonics are required to be slightly capacitive, which can help to absorb parasitic capacitance to achieve better matching results.

Considering the knee-point voltage and the finite harmonics of the voltage waveform, the efficiency of the NC-E PA is 80%. Giving an analytical solution to the generalised impedance space in Figure 2(d) is difficult, so the fitted form is used here instead:

$$\begin{cases} Z_{1f} = \left(1.285 + \left(0.97\lambda_1 + 0.93\right) j\right) R_{opt} \\ Z_{2f} = j\left(-1.72\lambda_1 - 2.26\right) R_{opt} \\ Z_{3f} = j\left(-0.6\lambda_1 - 1.69\right) R_{opt} \\ Z_{4f} = -1.15 j R_{opt} \\ Z_{5f} = -0.92 j R_{opt} \end{cases} \tag{26}$$

4 | NC-E PA DESIGN

CGH40010F basically satisfies $V_{knee} \approx 0.2V_{DC}$. Based on the continuous impedance space above, the design of the circuit is performed with this device. For this transistor, the optimal impedance can be calculated by the following equation:

$$R_{opt} = \frac{V_{DD} - V_{knee}}{I_{\max}/2} = \frac{28 - 0.2 \times 28}{1.5/2} = 29.9\Omega \tag{27}$$

Once R_{opt} is determined, its theoretical impedance space can be calculated with Equation 26. The parasitic parameters of the transistors also need to be taken into account in the design of output matching network (OMN), and the equivalent parasitic network (EPN) of the CGH40010F is shown in Figure 3(a)[10]. Considering the EPN, the load impedance at the transistor's intrinsic current generate (ICG) plane can be obtained[18]:

$$Z_{\mathrm{L}} = \frac{Z'_{\mathrm{OMN}}(1,1) \cdot 50 + Z'_{\mathrm{OMN}}(1,2)}{Z'_{\mathrm{OMN}}(2,1) \cdot 50 + Z'_{\mathrm{OMN}}(2,2)} \tag{28}$$

$$Z'_{\mathrm{OMN}} = Z_{\mathrm{EPN}} \cdot Z_{\mathrm{OMN}} \tag{29}$$

in which Z_{EPN} is the transferring matrix of the EPN, Z_{OMN} is the transferring matrix of the OMN. Besides, the Z_{OMN} can be obtained with the transferring parameters of the series/parallel stubs, and Z_{EPN} can be calculated using the specific parameters

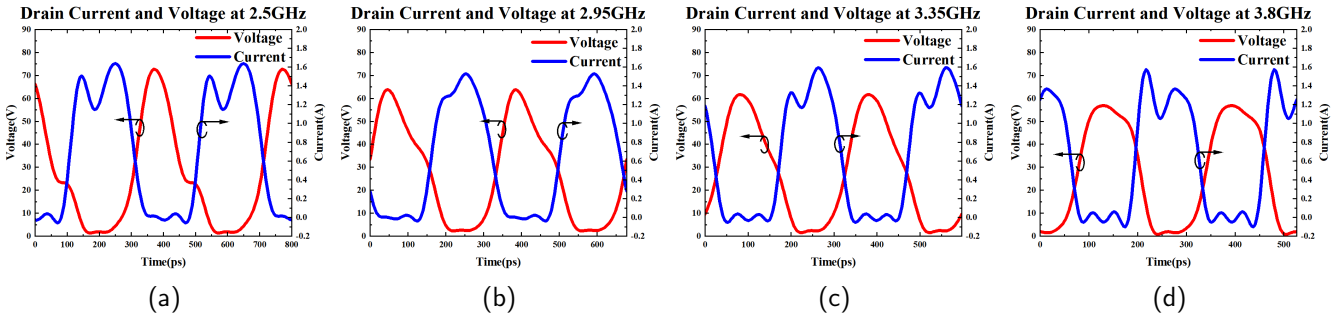

Figure 4 Simulated drain voltage and current waveforms in the current generate plane at: (a) 2.5GHz. (b) 2.95GHz. (c) 3.35GHz. (d) 3.8GHz.

of EPN, as:

$$Z_{\mathrm{EPN}} = \prod_{\mathrm{i}=1}^{3} \begin{bmatrix} 1 & 0 \\ j \cdot 2\pi \cdot f \cdot C_{\mathrm{i}} & 1 \end{bmatrix} \begin{bmatrix} 1 & j \cdot 2\pi \cdot f \cdot L_{\mathrm{i}} \\ 0 & 1 \end{bmatrix} \tag{30}$$

$$Z_{\mathrm{OMN}} = \prod_{\mathrm{i}=1}^{5} \begin{bmatrix} A_{\mathrm{TL}n} & jB_{\mathrm{TL}n} \\ jC_{\mathrm{TL}n} & D_{\mathrm{TL}n} \end{bmatrix} \tag{31}$$

where f is the frequency.

The network design method with dynamical continuous-mode criterions is used to build OMN network[21], and automatic circuit optimisation based on the ADS is conducted to realize the target design space in Equation 26. The designed OMN is shown in Figure 3(b). In terms of input matching, the Source-Pull technology is used to obtain the design space, and the input matching network design process is similar to that of OMN design. The final schematic of the total circuit is shown in Figure 3(c).

Figure 2(e) and Figure 2(f) show the idealized and simulated impedances of the designed PA at the intrinsic plane, where one can see that the design circuit achieves the desired impedance very well in fundamental and 2nd harmonic. For 3rd, 4th and 5th harmonics, it achieves the desired impedance basically, which is a compromise to achieve better 2nd harmonic matching. The properties of the theoretical impedance space lead to such a compromise, yet also allow matching at high order harmonics without sacrificing much circuit simplicity. In fact, other continuous modes such as continuous Class-F/F^{-1} do not have the advantage of high order harmonic matching, yet often need compromises in the matching of the 3rd harmonic as well[10,18,22,23]. Through layout simulation and de-embedding technology, the waveforms at the ICG plane are simulated in ADS, which are given in Figure 4. The simulated voltage waveforms are basically consistent with the theoretical waveform, but some current waveforms show a little clipping, which may be caused by the knee-point voltage[19].

5 | IMPLEMENTATION AND MEASUREMENT

The Rogers4350B substrate $\left(\varepsilon_{\mathrm{r}} = 3.66, \tan\delta = 0.0037\right)$ with a thickness of 20mil is used in fabrication of the microstrip circuit. Figure 3(b) shows the picture of the PA.

The produced PA is tested with a single tone signal and the input power is 30 dBm. Figure 5(d) shows the simulation and test values of the PA's PAE, DE, Pout and Gain performance. It can be seen that in the band of 2.5-3.8GHz, the DE is 66.2%∼74.2%, the output power is between 40.6dBm and 41.6dBm, and the gain is 10.6∼11.6dB. On the whole, an average DE of 70.8% and an average output power of 13.5W are achieved.

The PA is also tested with a two-tone signal with 5-MHz spacing at 2.5GHz, 3.15GHz ,3.8GHz. The measured carrier to the third-order intermodulation suppression ratio (C/IMD3) is better than -15.9 dBc at the three frequencies as shown in Figure 5(b).

Table 1 shows the performance comparison between the designed NC-E PA and other high-efficiency PAs published in recent years. These designs are manufactured with the same devices (CGH40010F). Overall, the NC-E PA achieves comparable bandwidth and efficiency. Besides, at high frequencies, its gain and output power performance are better than other designs with similar bandwidth and DE. This work have verifies the feasibility of the new theory.

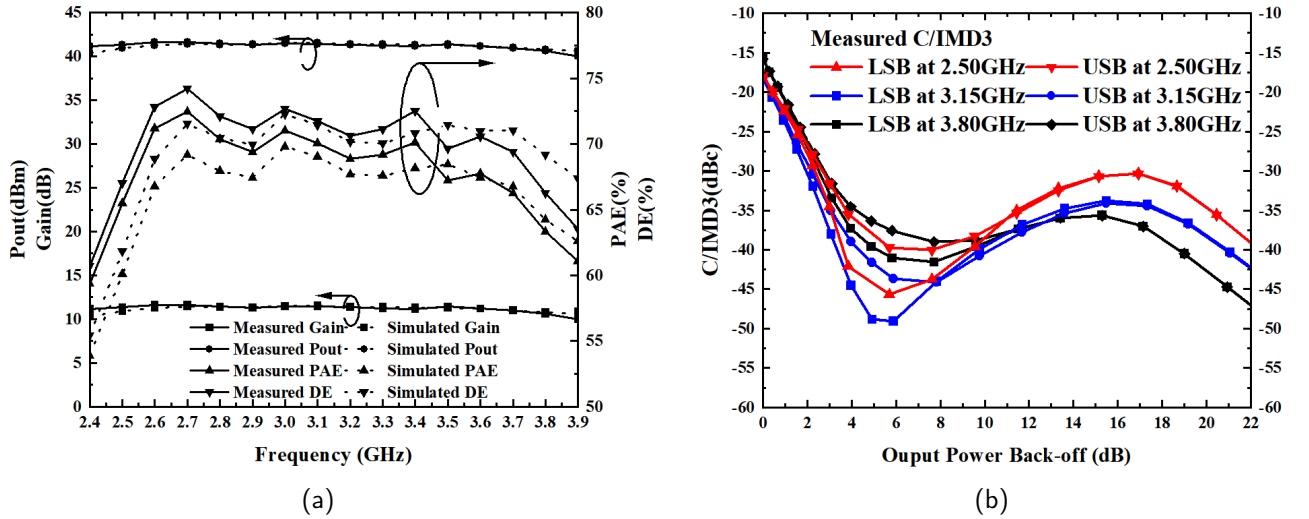

Figure 5 Performance of the fabricated PA. (a) PAE, DE, Gain, Pout performance versus frequency. (b) Measured C/IMD3 at 2.5GHz, 3.15GHz ,3.8GHz.

Table 1 Comparison of this PA and other published PAs.

Literature	PA mode	Device	Frequency(GHz)	Bandwidth(GHz)	Pout(dBm)	Gain(dB)	DE
2017[1]	E	CGH40010F	1.4-2.8	1.4(67%)	40-41.8	9-10.8	64-73
2017[9]	C-F	CGH40010F	1.5-2.5	1.0(50%)	39.5-41.5	9.5-12.7	60-75
2019[24]	E/F	CGH40010F	1.5-2.9	1.4(64%)	39.4-41.9	9.4-11.9	60.2-76.5
2020[25]	E/F	CGH40010F	1.7-2.6	0.9(42%)	38.8-40.5	10.8-13.7	68.5-81
2021[14]	E	CGH40010F	1.8-2.8	1.0(44%)	40-42.5	10-12.5	65-76
2022[26]	EF	CGH40010F	2.6-3.9	1.3(40%)	38.8-40.9	8.5-10.6	65-80.8
2022[27]	J*/B/J	CGH40010F	2-3	1.0(40%)	39-40.8	10-11.8	58-73.9
2022[10]	CCF	CGH40010F	3.3-4.3	1.0(26%)	39.9-40.3	/	55.9-65.3
This work	NC-E	CGH40010F	2.5-3.8	1.3(41%)	40.6-41.6	10.6-11.6	66.2-74.2

6 | CONCLUSIONS

This paper proposes a new general design theory for the high-efficiency broadband continuous PA, which is based on the solution of the high-efficiency equations. This new theory improves on the shortcomings associated with the CF and can be easily extent to other PAs. Subsequently, the theory is verified by using Class-E PAs' waveforms to achieve NC-E PAs. The NC-E PA has advantages in terms of broadband design and high order harmonic matching capability, which are more conducive to achieving target performance. Finally, a physical object using the NC-E PA's impedance space is designed and the test results show the effectiveness of the theory proposed in this paper.

References

1. Chen P, Yang K, Zhang T. Analysis and design of continuous class-E power amplifier at sub-nominal condition. *Int. J. Electron.* 2017; 104(12): 2007-2019. doi: 10.1080/00207217.2017.1335789

2. Thian M, Fusco VF. Transmission-Line Class-E Power Amplifier With Extended Maximum Operating Frequency. *IEEE Trans. Circuits Syst. II* 2011; 58(4): 195-199. doi: 10.1109/TCSII.2011.2124570

3. Yang W, Luo Y, Xuan D, Chang R, Hong G. A new harmonic tuned class E power amplifier based on waveform analysis. *Int. J. Circ. Theor. Appl.* 2022; 50(6): 1890-1906. doi: https://doi.org/10.1002/cta.3259

4. Saad P, Fager C, Cao H, Zirath H, Andersson K. Design of a Highly Efficient 2-4GHz Octave Bandwidth GaN-HEMT Power Amplifier. *IEEE Trans. Microw. Theory Tech.* 2010; 58(7): 1677-1685. doi: 10.1109/TMTT.2010.2049770

5. Mary Asha Latha Y, Rawat K. Extending the Design Space of Class E Mode to Design a Multi-Octave Power Amplifier. *IEEE Transactions on Circuits and Systems II: Express Briefs* 2022; 69(12): 4829-4833. doi: 10.1109/tcsii.2022.3195730

6. Moloudi F, Eslamipour O. Wide-band switching-mode power amplifier using varactor-based reconfigurable output matching network. *AEU - International Journal of Electronics and Communications* 2021; 132. doi: 10.1016/j.aeue.2021.153647

7. Woo YY, Yang Y, Kim B. Analysis and experiments for high-efficiency class-F and inverse class-F power amplifiers. *IEEE Trans. Microw. Theory Tech.* 2006; 54(5): 1969-1974. doi: 10.1109/TMTT.2006.872805

8. Kim JH, Jo GD, Oh JH, Kim YH, Lee KC, Jung JH. Modeling and Design Methodology of High-Efficiency Class-F and Class- F^{-1} Power Amplifiers. *IEEE Trans. Microw. Theory Tech.* 2011; 59(1): 153-165. doi: 10.1109/TMTT.2010.2090167

9. Aggrawal E, Rawat K, Roblin P. Investigating Continuous Class-F Power Amplifier Using Nonlinear Embedding Model. *IEEE Microw. Wirel. Compon. Lett.* 2017; 27(6): 593-595. doi: 10.1109/LMWC.2017.2701316

10. Sadeque MG, Yusoff Z, Hashim SJ, Marzuki ASM, Lees J, FitzPatrick D. Design of Wideband Continuous Class-F Power Amplifier Using Low Pass Matching Technique and Harmonic Tuning Network. *IEEE Access* 2022; 10: 92571-92582. doi: 10.1109/access.2022.3202886

11. Ozen M, Jos R, Fager C. Continuous Class-E Power Amplifier Modes. *IEEE Trans. Circuits Syst. II* 2012; 59(11): 731-735. doi: 10.1109/TCSII.2012.2228392

12. Almeida dJV, Wu K. Theory of continuous inverse class-E power amplifier modes and continuous-mode self-distortion. *Microwave and Optical Technology Letters* 2021; 63(8): 2165-2170. doi: https://doi.org/10.1002/mop.32878

13. Ortega-Gonzalez FJ. Load-Pull Wideband Class-E Amplifier. *IEEE Microw. Wirel. Compon. Lett.* 2007; 17(3): 235-237. doi: 10.1109/LMWC.2006.890504

14. Wei LY, Zhang ZB, Chen FC. Design of Efficiency-Enhanced Wideband Power Amplifiers Based on Novel Matching Network with Controllable Transmission Zeros. In: 2021 Cross Strait Radio Sci. Wir. Tech. Conf. (CSRSWTC). ; 2021.

15. Chen K, Peroulis D. Design of Broadband Highly Efficient Harmonic-Tuned Power Amplifier Using In-Band Continuous Class- F^{-1}/F Mode Transferring. 2012; 60(12): 4107-4116. doi: 10.1109/TMTT.2012.2221142

16. Qi C, Luo Y, Feng X, Dong C. 1.6-2.6GHz continuous Class-F power amplifier with gain and power-added efficiency flatness enhancement by negative feedback structure. *Microwave and Optical Technology Letters* 2019; 61(7): 1716-1722. doi: https://doi.org/10.1002/mop.31804

17. Tuffy N, Guan L, Zhu A, Brazil TJ. A Simplified Broadband Design Methodology for Linearized High-Efficiency Continuous Class-F Power Amplifiers. *IEEE Transactions on Microwave Theory and Techniques* 2012; 60(6): 1952-1963. doi: 10.1109/tmtt.2012.2187534

18. Han K, Geng L. Enhancing Efficiency and Linearity of Continuous Class-F₃ Power Amplifier With Peak-Clipped Current Waveform. *IEEE Transactions on Microwave Theory and Techniques* 2022; 70(2): 1423-1431. doi: 10.1109/tmtt.2021.3135499

19. Cripps S. RF Power Amplifiers for Wireless Communications, Second Edition. 2006: 59-60.

20. Raab F. Idealized operation of the class E tuned power amplifier. *IEEE Trans. Circuits Syst.* 1977; 24(12): 725-735. doi: 10.1109/TCS.1977.1084296

21. Han K, Geng L. Design of 0.6–0.8-GHz and 1.6–1.9-GHz Dual-Band PA With Peak PAEs of Over 70 by NPE Method With Dynamical Continuous-Mode Criteria. *IEEE Microwave and Wireless Components Letters* 2021; 31(7): 873-876. doi: 10.1109/lmwc.2021.3074965

22. Lu Z, Chen W. Resistive Second-Harmonic Impedance Continuous Class-F Power Amplifier With Over One Octave Bandwidth for Cognitive Radios. *IEEE Journal on Emerging and Selected Topics in Circuits and Systems* 2013; 3(4): 489-497. doi: 10.1109/jetcas.2013.2284615

23. Chen H, Xu JX, Kong ZH, Chen WH, Zhang XY. Broadband High-Efficiency Power Amplifier With Quasi-Elliptic Low-Pass Response. *Ieee Access* 2020; 8: 52566-52574. doi: 10.1109/Access.2020.2980688

24. Mary Asha Latha Y, Rawat K, Roblin P. Nonlinear Embedding Model-Based Continuous Class E/F Power Amplifier. *IEEE Microw. Wirel. Compon. Lett.* 2019; 29(11): 714-717. doi: 10.1109/LMWC.2019.2941919

25. Yang Z, Li M, Dai Z, et al. A Generalized High-Efficiency Broadband Class-E/F3 Power Amplifier Based on Design Space Expanding of Load Network. *IEEE Trans. Microw. Theory Tech.* 2020; 68(9): 3732-3744. doi: 10.1109/TMTT.2020.3009530

26. Liu C, Zhang H, Chen W, Ghannouchi FM. Novel Design Space of Broadband High-Efficiency Parallel-Circuit Class-EF Power Amplifiers. *IEEE Trans. Circuits Syst. I* 2022; 69(9): 3465-3475. doi: 10.1109/TCSI.2022.3177283

27. Lavandera-Hernandez I, Loo-Yau JR, Reynoso-Hernandez JA, Ochoa-Armas D, Moreno P. Frequency-Dependent Design Spaces for Continuous Mode Class-J*/B/J PA. *IEEE Transactions on Circuits and Systems I: Regular Papers* 2023; 70(1): 203-213. doi: 10.1109/tcsi.2022.3208826